Results from a full coupling of the HIRHAM regional climate model and the MIKE SHE hydrological model for a Danish catchment

Morten A. D. Larsen, Department of Geosciences and Natural Resource Management, University of Copenhagen, Øster Voldgade 10, DK-1350 Copenhagen, Denmark. Email: madla@dtu.dk.
Jens C. Refsgaard, Geological Survey of Denmark and Greenland, Øster Voldgade 10, DK-1350 Copenhagen, Denmark.
Martin Drews, Department of Management Engineering, Technical University of Denmark, Risø Campus, Frederiksborgvej 399, DK-4000 Roskilde.
Michael B. Butts, DHI, Agern Alle 5, DK-2970, Hørsholm, Denmark
Karsten H. Jensen, Department of Geosciences and Natural Resource Management, University of Copenhagen, Øster Voldgade 10, DK-1350 Copenhagen, Denmark.
Jens Hesselbjerg Christensen, Danish Meteorological Institute, Lyngbyvej 100, DK-2100 Copenhagen Ø Denmark.
Ole Bøssing Christensen, Danish Meteorological Institute, Lyngbyvej 100, DK-2100 Copenhagen Ø Denmark.

Abstract

A major challenge in the emerging research field of coupling of existing regional climate models and hydrology/land-surface models is the computational interaction between the models. Here we present results from a full two-way coupling of the HIRHAM regional climate model over a 4000 km x 2800 km domain at 11 km resolution and the combined MIKE SHE-SWET hydrology and land-surface models over the 2500 km^2 Skjern river catchment. A total of 26 one-year runs were performed to assess the influence of the data transfer interval (DTI) between the two models and the internal HIRHAM model variability of ten variables. DTI frequencies between 12-120 min were assessed, where the computational overhead was

found to increase substantially with increasing exchange frequency. In terms of hourly and daily performance statistics the coupled model simulations performed less accurately than the uncoupled simulations whereas for longer term cumulative precipitation the opposite was found especially for more frequent DTI rates. Four of six output variables from HIRHAM, precipitation, relative humidity, wind speed and air temperature, showed statistically significant improvements in root-mean-square-error (RMSE) by reducing the DTI. For these four variables, the HIRHAM RMSE variability corresponded to approximately half of the influence from the DTI frequency and the variability resulted in a large spread in simulated precipitation. Conversely, DTI was found to have only a limited impact on the energy fluxes and discharge simulated by MIKE SHE.

1 – Introduction

Combined modelling of atmospheric, surface and subsurface processes has been performed in a broad range of studies over the years utilizing increasingly complex model codes. For example, by coupling vegetation and hydrological processes using the Lund–Potsdam–Jena vegetation model (LPJ GUESS), Gerten et al. (2004) obtain more realistic global reproductions of evapotranspiration and runoff as compared to a stand-alone hydrological model and argue that the coupling with vegetation processes may account for rising CO_2 levels not simulated using hydrological models alone. Similarly Yan et al. (2012) successfully simulate global evapotranspiration with an energy based vegetation and water balance land-surface model, while Anyah et al. (2008) show a direct connection between soil moisture and simulations of evapotranspiration over the Western North America, where soil water is a limiting factor. Several studies deal with the influence of surface hydrology, vegetation and land use change on atmospheric processes. Seneviratne et al. (2006) show that land-atmosphere coupling processes are significant in representing the variability of temperature projections for 2070 to 2099. Zeng et al. (2003) highlight the considerable influence of land-surface temperature and moisture heterogeneities on simulations of sensible (H) and latent heat (LE) fluxes as well as the precipitation pattern, using the RegCM2 regional climate model. Cui et

al. (2006) show a substantial change in ECHAM5 general circulation model predictions as a consequence of projected changes in vegetation. Kunstmann and Stadler (2005), Smiatek et al. (2012) and York et al. (2002) study the influence of the atmosphere on land-surface and subsurface state. Of these, York et al. (2002) use the CLASP II model with coupled aquifer-atmosphere processes for a single grid box to study the response of groundwater levels to climate forcing.

Current climate models include only a simplistic surface and subsurface description of hydrology processes and similarly hydrological models generally include atmospheric processes in a surface-near layer in the scale of meters. More recent studies have therefore focused on combining model codes that each represents a component in the total simulation of atmospheric, land-surface and subsurface processes as well as ocean processes. Of these, a few studies have focused on coupling a mesoscale atmospheric model with a combined land-surface and hydrological model. Maxwell et al. (2007) for example study the coupling of the ARPS mesoscale atmospheric model (*Xue et al*., 2000, 2001) and the ParFlow hydrological model (Kollet and Maxwell, 2008) for a 36 hour period over the Little Washita catchment in Oklahoma, USA. Rihani (2010) uses the same combination of models and catchment to address the effects of terrain, land cover etc. for a period of 4 days. In Maxwell et al. (2011) ParFlow is coupled with the WRF atmospheric model (Skamarock et al., 2008) and the NOAH land-surface model (Ek et al., 2003) for 48 hour idealized and semi-idealized runs and in Jiang et al. (2009) WRF is coupled with NOAH and the simple SIMGM groundwater model. A recent study utilizes a fully dynamic coupling of the COSMO atmospheric model, the CLM3.5 land-surface model and the ParFlow hydrology model for a one week summer period (Shresta et al. 2014). Furthermore, a few recent studies couple atmospheric models in climate mode, i.e. performing longer term simulations at larger spatial scales. Rasmussen (2012) for example studied the HIRHAM regional climate model (Christensen et al., 2006) and the MIKE SHE hydrological model (Graham and Butts, 2005) with the SWET land-surface scheme (Overgaard, 2005) in one-way coupled mode, where output from the regional climate model is transferred to the hydrological model over the FIFE test domain in Kansas, USA, for the period May to October 1987. In that study, data are exchanged over an area represented by a

single 0.125 degree HIRHAM grid cell. In two more recent studies, the MM5 regional climate model and the PROMET land-surface model (Zabel and Mauser, 2013) and the CAM atmosphere model and the SWAT hydrology model (Goodall et al., 2013) have been coupled.

A comprehensive two-way coupling between the HIRHAM regional climate model and the MIKE SHE hydrological model combined with the SWET land-surface model for the 2500 km^2 Skjern river catchment in Denmark has recently been established by Butts et al. (submitted) and used for a one-year simulation. To our knowledge, no previous studies have been reported on long term simulations (more than a few days) employing couplings between a distributed regional climate model and a full 3D groundwater-surface water hydrological model for catchments larger than a single regional climate model grid point. A limitation of the study of Butts et al. (submitted) is the need to understand the influence of the data transfer interval (DTI) between the two models, an issue which has also not been reported in previous studies.

Another crucial issue, when systematically evaluating climate model results, is the inherent model variability where minor changes to the model setup, induced either by artificially perturbing initial conditions (Giorgi and Bi, 2000) or by altering the domain location (Larsen et al., 2013) result in significant variations in the simulated atmospheric variables. Giorgi and Bi (2000) show for regions in China that especially during the summer and for high precipitation events, precipitation is highly sensitive to perturbations in the initial and boundary conditions. Similarly, Alexandru et al. (2007) used the Canadian regional climate model CRCM (Caya and Laprise, 1999) over five domains with twenty perturbed runs for each domain to assess model variability in precipitation. They found at least 10 ensemble members were needed to reproduce the correct seasonal means although this number is dependent on the domain size.

In this paper we study the interaction and feedback mechanisms between the atmosphere and the land surface by two-way coupling of proven climate and hydrology models each operating in an environment where the other model component deliver high quality boundary conditions using the same setup as Butts et al. (submitted). Our hypothesis is that the inclusion of feedback will provide a significantly changed signal when compared to uncoupled simulations. In addition, the current study aims to evaluate the influence of

101 the data transfer interval (DTI) between the two models since this strongly influences computation time
102 and to evaluate the importance of the internal HIRHAM model variability by assessing the sensitivity of the
103 simulation results to perturbations of boundary and initial conditions.
104
105 **2 – Method**
106 **2.1 – Study area**
107 The climate and hydrological models used in this study each cover areas typical of their application range.
108 The HIRHAM regional climate domain model covers an area of approximately 2800 km x 4000 km from
109 northwest of Iceland to southern Ukraine (figure 1). Approximately 60% of the latitudinal stretch is located
110 west of the Skjern catchment where most local weather systems originate. The MIKE SHE model setup
111 covers the Skjern catchment area of 2500 km^2 (figure 1) located in the western part of the Jutland
112 peninsula. The data exchange between the models occurs at the overlapping grid cells with the hydrological
113 catchment nested within the climate model domain (figure 1). Skjern River emerges in the central Jutland
114 ridge at approx. 125 m above sea level and has its outlet into the Ringkøbing fjord. The Jutland ridge has a
115 maximum elevation of approx. 130 m. Two general soil classes can be distinguished within the catchment;
116 sandy soils generated by the Weichsel ice age glacial outwash and till soils from the previous Saalian ice
117 age. The catchment land use is divided between 61% agriculture, 24% meadow/grass/heath, 13% forest
118 and 2% other. For the period 2000-2009 the average annual measured precipitation is 940 mm, which
119 when corrected for turbulence related gauge undercatch (Allerup et al., 1998) amounts to 1130 mm/year.
120 The mean annual air temperature for the same period is 9.3 ^{o}C.
121
122 **2.2 – Observed input and validation data**
123 Measurements from three sites having flux towers, placed over agricultural, meadow and forest surfaces,
124 respectively, are used for calibration of the hydrological model (figure 1) as described in Larsen et al.
125 (submitted). At these locations we have measurements of latent (LE), sensible (H), and soil heat fluxes (G),

126 radiation components, soil/air temperature, precipitation, wind speed, soil moisture and groundwater
127 table depth. The latent and sensible heat fluxes are measured above the vegetation using eddy-covariance
128 sonic anemometers and the soil heat flux is measured using hukseflux plates at 5 cm depths. Latent and
129 sensible heat fluxes are gap-filled and corrected according to data quality using the Alteddy software 3.5
130 (Alterra, University of Wageningen, the Netherlands) as described in Ringgard (2012). Up to 45% of the data
131 is replaced. For the periods 21 July-16 August and 24 August-28 October in 2009, no data were recorded at
132 the agricultural site and were therefore replaced by data from the forest site (Ringgaard et al. 2011).
133 Discharge measurements (Q) from the three discharge stations Ahlergaarde (1055 km^2), Soenderskov (500
134 km^2) and Gjaldbaek (1550 km^2) were also used for calibrating the hydrological model (Larsen et al.,
135 submitted) and in the present study for point validation (figure 1).
136 To drive the MIKE SWET module six climatic variables are needed. Daily precipitation (PRECIP) data are
137 derived from gauge stations and interpolated by kriging to a 500 m grid as described in Stisen et al. (2011a).
138 The precipitation data are dynamically corrected for gauge undercatch (Allerup et al., 1998 and Stisen et al.,
139 2011b). The remaining five variables; air temperature (Ta), wind speed (V), relative humidity (RH), surface
140 pressure (Ps) and global radiation (Rg) are based on measurements from climatic stations. The data have
141 been interpolated in space and time to produce hourly datasets at a 2 km resolution (Stisen et al., 2011b).
142 For the assessments made here, these six distributed variables have been bi-linearly interpolated to match
143 the exact grid of the HIRHAM setup allowing for grid-by-grid calculations.
144
145 **2.3 – MIKE SHE**
146 In the present study we use the MIKE SHE hydrological model that represents all key hydrological processes
147 in the land-surface part of the hydrological cycle such as evapotranspiration, snow melt, channel flow (the
148 MIKE 11 component), overland flow, unsaturated flow, saturated flow as well as irrigation and drainage
149 (Graham and Butts, 2005).

The SWET component is included to handle the vegetation and energy balance processes occurring in the land-surface interface from the root zone and into the lower atmospheric boundary layer (Overgaard, 2005). The SWET model is based on a two-layer system with resistances for both soil and canopy, as presented in Shuttleworth and Wallace (1985), but modified to include energy fluxes from ponded water and vegetation interception storage (Overgaard, 2005). A limitation to the current SWET model is that snow accumulation/melt is not yet included, which may be important under Danish conditions.

In the current setup, the MIKE SHE model is derived from the Danish national water resources model (DK-model) (Stisen et al., 2011a, 2012; Højberg et al., 2013) at 500 m resolution. The model setup includes 11 computational layers in the groundwater system and an extensive river network and is implemented with a basic (maximum) time step of 1 hour, which is reduced dynamically during precipitation events.

2.4 – HIRHAM

The climate model used in the present coupling study is the HIRHAM regional climate model version 5 (Christensen et al., 1996; Christensen et al., 2006). HIRHAM is based on the atmospheric dynamics from the HIRLAM model used for operational weather forecasting (Undén et al., 2002) and physical parameterization schemes from the ECHAM5 general circulation model (Roeckner et al., 2003). HIRHAM is a hydrostatic model and typically implemented in resolutions of 5-50 km, here applied at a resolution of 11 km on a rectangular grid. The HIRHAM model is here driven by ERA-Interim reanalysis data as lateral boundary conditions (Uppala et al., 2008), and the internal model time step is 120 sec. The derivation of the domain is described in Larsen et al. (2013).

2.5 – Coupling code

A challenge in developing the coupling code used for this work is that the MIKE SHE and HIRHAM models operate on different computing platforms, i.e. a Windows workstation and a highly parallelized Linux supercomputing facility, respectively. To facilitate communication across these very different platforms, an

175 Open Modelling Interface (OpenMI, www.openmi.org) code have therefore been developed and used on
176 the Windows workstation side, and MIKE SHE was modified to exploit OpenMI. On the Linux side
177 modifications to the HIRHAM code were made and additional code controlling the data exchange
178 developed. An OpenMI interface was installed in order to facilitate the communication between existing
179 time-dependent model codes running simultaneously and to handle differences in time step, model
180 domain, resolution and discretization (Gregersen et al., 2005; Gregersen et al., 2007).
181 The OpenMI and Linux/HIRHAM coupling code served four general functions: 1) To control the timing
182 between models so that data are stored from one model waiting for the other to reach the point in time of
183 specified data exchange. 2) To define which variables to be exchanged in both directions and to handle
184 potential unit conversion factors, offsets and aggregation types. 3) To handle the spatial grid structure of
185 each model and transfer the data based on a selected spatial interpolation mapping. 4) To collect and
186 interpolate data for each separate model time step to be exchanged between models at each data
187 exchange time step, based on the differing time steps in the two model codes, including MIKE SHE's
188 dynamically varying time steps during precipitation events.
189 As both modelling platforms include numerous variables in two or three dimensions, the exchange of data
190 between the models are selected within the modelling scope of using the HIRHAM climate forcing as input
191 to MIKE SHE/SWET as well as transferring energy and water fluxes in the opposite direction. The exchange
192 of data between the models is as follows: (1) MIKE SHE receives the driving variables: PRECIP, RH, V, Rg, Ta
193 and Ps from HIRHAM, and (2) HIRHAM receives the variables LE and surface temperature (Ts) from MIKE
194 SHE. Ts is then used to calculate H within the HIRHAM code. The spatial mapping in this study was based on
195 a weighted mean method where each grid cell contributes relatively according to the land share fraction.
196 In the current version of the coupling LE and Ts (and therefore H) calculated by MIKE SHE directly replaces
197 the corresponding variables within HIRHAM one-to-one over the shared domain, whereas outside of the
198 domain the simple land surface scheme embedded in the regional climate model is preserved.
199 Atmospheric fields are then updated based on the modified surface energy balance from MIKE SHE. In this

study no means are implemented to assure ensuing internal physical consistency of fields within HIRHAM. Therefore, effects directly related to differences in spatial and temporal scales and in the physical formulation of the land surface scheme may be found along the boundary of the hydrological catchment. The boundary effects seen here are however relatively small, which again to a large degree is due to differences in spatial and temporal scales, i.e. to cell averaging and cancellation of errors when feeding the MIKE SHE surface back to HIRHAM. In this work we address primarily the effect of the temporal scale differences on the coupled system i.e. by varying DTI.

The standard OpenMI method for data exchange is memory-based. However, due to local safety regulations for network data exchange at the location of model execution, the current setup is constrained to the exchange of data files on a shared drive visible to both the Windows and Linux model setups. Naturally, this network file transfer generates a significant overhead with respect to execution time when data exchange is frequent, which by far exceeds that of the added overhead on each of the individual models.

2.6 – Simulations

All model simulations were performed for the one-year period from 1 May 2009 to 30 April 2010 with a spin-up period from the beginning of March to 30 April 2009. A total of 26 model runs were used; in the present study they are divided into four main categories (see also table 1):

- Transfer interval (TI): Eight two-way fully coupled simulations were performed by varying the data transfer interval (DTI), between the HIRHAM and MIKE SHE models, between 12 and 120 min. These DTI values were chosen to conform to time step restrictions imposed by MIKE SHE (given in fractions of an hour) to ensure accurate process modelling and to allow for executing model runs within the time slots allocated by DMI's supercomputing facility. The TI runs used 1 March 2009 as starting day.

- HIRHAM uncoupled variability (HUV): Eight HIRHAM uncoupled simulations were performed each starting one day apart from 1 March to 8 March 2009.
- Coupled variability (CV): Eight two-way fully coupled simulations using a 60 min DTI were performed using starting dates from 1 March to 8 March 2009 as above.
- MIKE SHE data source (MSDS): To assess the influence of data sources on MIKE SHE performance two MIKE SHE simulations were performed. (1) Uncoupled mode using observed values of PRECIP, RH, V, Rg, Ta and Ps and (2) One-way coupled mode using simulated values as driving variables based on HIRHAM model simulations with 30 min DTI and without feedback to HIRHAM.

The eight uncoupled HIRHAM runs all show varying geographical and temporal patterns of, in particular, precipitation. With these changes in precipitation, the water available for evapotranspiration and the energy balance is altered, and therefore attention should be given to which simulations are compared. For all models runs, simulation output from HIRHAM were assessed for the six climatic variables PRECIP, RH, V, Rg, Ta and Ps since observations were available. The same observational data were also used as input to MIKE SHE SWET for the uncoupled runs. Likewise, the output from the MIKE SHE simulations was assessed by comparing to measurements of LE, H and G at the agricultural, forest and meadow sites (figure 1) as well as discharge measurements from three gauging stations.

Figure 2 outlines the data flow and simulation categories. As the Skjern Catchment has an irregular shape, different degrees of overlap are found between the HIRHAM grid cells and the hydrological catchment (figure 1). Analyses of PRECIP, RH, V, Rg, Ta and Ps were therefore performed for five domains that reflect these different degrees of overlap;

- Dom1: Cells with 100% overlap (9 cells)
- Dom2: Dom1 + the cells with 50-100% overlap (23 cells)
- Dom3: Dom2 + the cells with 0-50% overlap (30 cells)
- Dom4: Dom3 + cells located immediately downstream of the catchment with regards to the dominant western wind direction (42 cells)

- Dom5: A cluster of cells east of the coupled catchment (4 cells)

For HIRHAM output, the evaluation was performed on all five test domains by calculating a single root mean square error (RMSE) value for each full model simulation. For MIKE SHE output, the RMSE was performed on the point data only. The RMSE was calculated on the basis of hourly values of RH, V, Rg, Ta, Ps, LE, H and G and daily values of PRECIP and Q against the corresponding observations for the six HIRHAM and four MIKE SHE variables:

$$RMSE = \sqrt{\frac{\sum_{i,t}(SIM_{i,t} - OBS_{i,t})^2}{n}} \quad (1)$$

where SIM and OBS are simulated and observed values respectively, i and t are location and time respectively, and n is the total number of data points. To assess the output variability from each of the three simulation groups involving HIRHAM (TI, CV and HUV), simulation box plots with the 25th and 75th percentiles including whiskers for the most extreme data were created (figure 5 and 8).

Similarly, the mean absolute errors (MAE) were assessed to gain more information on the expected improvements for simulations with a more frequent DTI:

$$MAE = \frac{\sum_{i,t}|SIM_{i,t} - OBS_{i,t}|}{n} \quad (2)$$

where the terms correspond to the RMSE calculations. The MAE calculations, for the TI simulations, were performed for each of the six HIRHAM variables over each of the five test domains and the four MIKE SHE variables at point scale. Linear trend lines, using least squares, were then fitted to the 12-120 min DTI MAE values for each of the test domains and point scale output and for each variable. The mean absolute and percentage change in MAE, based on the trend lines from the 120 min to the 12 min data points, were then calculated. Also, correlation coefficients on the basis of the trend lines were calculated to detect statistical significance at a 95% two-tailed level.

The HUV and CV simulation groups apply the same changes in initial conditions by using different start dates to perturb these initial conditions but differ by having different land surface schemes over the Skjern

catchment. These simulations were therefore used to test for statistical significance of the coupling. A simple two-sample t-test was performed for each of the test domains and variables for the HUV and CV simulations to test the hypothesis of these simulation groups having unequal means.

3 – Results

3.1 – HIRHAM output

3.1.1 - Data transfer interval (DTI)

Of the six HIRHAM output variables, the four variables of PRECIP, RH, V and Ta show a significant decrease in RMSE with decreasing DTI in the fully two-way coupled mode simulations, whereas Ps is less affected and Rg is unaffected (figure 3). Based on the linear trend line averages between the domains, RMSE improvements of 1.1 mm/day, 1.1%, 0.2 m/s and 0.3 ^{o}C are seen for PRECIP, RH, V and Ta respectively (table 2). Similarly, MAE shows improvements of 0.3 mm/day, 0.8%, -0.1 m/s and 0.2 corresponding to a change from the 120 to the 12 min simulations of 7.2% averaged for the four significant variables (table 2). For the variables with statistically significant trends, PRECIP, RH, V and Ta, there is a specific order in the resulting RMSE trend line locations with the largest RMSE values for Dom1, Dom2 etc., decreasing down to Dom5.

The execution time for the coupled setup, as a function of DTI, is shown in figure 4. Only a moderate increase in execution time is seen in the range of 60-120 min DTI values whereas a sharp increase is seen from DTI values of around 15-30 min.

3.1.2 – HIRHAM model variability

Figure 5 shows the output variability for each of the TI, CV and HUV group runs for each of the five test domains, Dom1-Dom5. For PRECIP, RH, V and to some extent Ta, the largest variability is seen for the two-way coupled runs (TI). The RH and V, using a 60 min DTI, for both the coupled (CV) and uncoupled (HUV) runs show almost negligible variability. For PRECIP and Ta, the largest variability is seen for the CV

297 simulations for PRECIP whereas the opposite is seen for Ta with a larger variability in the HUV simulations.
298 For the variables, PRECIP, RH, V and Ta, a general decrease in RMSE is seen for the coupled TI and CV
299 simulations with increasing test domain number from Dom1 to Dom5. For the HUV simulations, this pattern
300 is seen, to some extent, for PRECIP only. The Rg and Ps variables show comparable levels of variability
301 between the TI, CV and HUV simulations groups. For Rg, the RMSE values increase with test domain
302 number whereas the opposite is the case for Ps.
303 The range in RMSE values from the perturbation induced HUV variability corresponds to 47% of the RMSE
304 improvement for the TI simulations when going from 120 to 12 min (based on the linear trend lines). The
305 corresponding number when comparing TI with CV is 46%.
306 Two-sample t-tests confirmed the hypotheses that the results from the HUV and CV simulations belong to
307 two separate populations for the variables PRECIP, RH, V and Ta with significance levels of 98.2% or above.
308 For these four variables, there was a clear pattern of decreasing significance with increasing test domain
309 number corresponding to a lesser degree of coupling.
310 Figure 6 shows the simulated PRECIP for each run, for each of the TI, HUV and CV simulation groups and for
311 each test domain. PRECIP is seen to decrease with increasing domain number for all three simulation
312 groups. This decrease is strongest for the two-way coupled TI and CV simulation groups which also show
313 the highest PRECIP levels compared to the uncoupled HUV simulations. Compared to the observed PRECIP
314 mean over the five test domains of 892 mm over the simulation period, both the TI and CV simulations
315 consistently overestimate PRECIP with accumulated values of 1004 mm and 1027 mm respectively. In
316 contrast, the HUV underestimates the PRECIP for this period, with an accumulated value of 868 mm.
317 Despite generally overestimating the rainfall, the coupled TI runs, with high frequency DTIs and a high
318 degree of coupling (Dom1-Dom3), show better estimates of accumulated rainfall compared to uncoupled
319 run (CV). With regard to timing there is a tendency for the main part of the TI simulation variability to arise
320 from events in the fall months of 2009 whereas most of the HUV and CV variability occurs in early 2010
321 events.

In addition to comparing simulation statistics and precipitation accumulation plots, the HIRHAM output variables for all 24 TI, HUV and CV simulations are plotted in figure 7. This figure shows hourly values for the period 10 July-17 July, 2009, with the exception of precipitation data which are given as daily values for all of August, 2009. A large spread is seen for precipitation amounts on individual days that appears to increase with the mean intensity, most pronounced on 10 and 20 August. Reasonable agreement is seen between these simulations in terms of capturing the dry days. For the remaining five variables, RH, Ta, Ps and especially V and Rg, the period with low pressure and precipitation, 10 July to 12 July, exhibits a fair amount of spread between the individual simulations, whereas the remaining period, 13 July to 17 July, shows a higher degree of consistency within each simulation group (TI, HUV and CV) especially in terms of dynamics. For the PRECIP, RH, V and Ta variables the coupled simulations groups of TI and CV clearly deviate from the HUV simulations in terms of the timing, dynamics and absolute levels. Of these, the most noticeable difference is the daytime RH and night time Ta, which are notably higher and lower, respectively, for the HUV simulations.

3.2 – MIKE SHE output

As for the HIRHAM simulations, the MIKE SHE RMSE results are plotted as a function of DTI (figure 8). LE shows a general improvement in RMSE with a higher frequency of exchange (smaller DTI), which is strongest for the agriculture and forest sites. Correlation coefficients between RMSE and DTI of 0.83, 0.55 and 0.13 are found for the agriculture, forest and meadow sites respectively. Conversely, H shows general decreases in RMSE with increased DTI and with correlation coefficients of -0.80 to -0.83. The changes in LE and H thereby represent opposing signals which could be expected, to some degree, from the conservation of the energy balance. No clear trend between DTI and RSME results is seen for both G and Q and the corresponding correlation coefficients are generally low.

For LE, an absolute improvement of 1.9 W/m^2 in both MAE and RMSE is seen from the 120 to 12 min trend line average data points corresponding to 6.9% and 4.5% for MAE and RMSE respectively (table 2). Overall

347 the one-way coupled and uncoupled MSDS simulations are superior to the TI simulations with the
348 exception of agricultural LE and G and meadow G. The HIRHAM climate model variability as represented by
349 the CV simulations produces a resulting MIKE SHE RMSE total output span of 1.5 W/m^2, 1.5 W/m^2, 0.7
350 W/m^2 and 2.2 m^3/s for LE, H, G and Q as an average of the three surfaces and the three discharge stations
351 (figure 8). By comparison the TI simulations induce a spread in the corresponding results, not based on the
352 trend lines as in table 2, of 3.7 W/m^2, 3.8 W/m^2, 4.5 W/m^2 and 1.3 m^3/s, respectively.
353 The variations in the MIKE SHE output for four variables LE, H, G and Q, for the CV and TI model runs, are
354 shown in figure 9. Also here there is no distinct pattern distinguishing the TI and CV simulation group
355 results. The simulations for 10-12 July show larger variations in simulated fluxes reflecting the variability in
356 the HIRHAM simulations. Using either observation data as driving input for MIKE SHE or the HIRHAM data
357 (i.e. the MSDS runs) however resulted in substantial variations in the results. As expected due to the change
358 in forcing data, the uncoupled (observation data input) runs resulted in shifts in LE, H and G values for both
359 peaks (day time) and lows (night time) most obvious for G. The one-way coupled run output (HIRHAM data
360 input) seems to provide better match than when based on observation data, especially for night time LE
361 and G, than the TI and CV runs. It should be pointed out that for this analysis (figure 9), that although
362 results are extracted from three single MIKE SHE cells (for meadow, forest and agriculture), the forcing data
363 are based on either 11 km resolution HIRHAM data input (TI and CV) or 10 km observation gridded data
364 (station interpolated – MSDS), which can be expected to smooth out local features.
365
366 **4 – Discussion**
367 The motivation for performing this coupling study is to include the land-surface-atmosphere interactions
368 between the RCM and the hydrological model. Our hypothesis is that the RCM will benefit from the more
369 detailed representation of the surface and subsurface processes provided by the dedicated hydrological
370 model as compared to the much simpler land-surface schemes that climate models usually rely on.
371 Similarly, we expect that the hydrological model would benefit from the better representation of the

horizontal redistribution processes in the atmosphere offered by the dynamic coupling with the climate model.

4.1 - Performance of coupled versus uncoupled model

As shown above, the performance of the coupled model simulations (TI and CV) when compared to hourly values of RH, V and Ta and daily PRECIP, is generally poorer than the uncoupled model simulations (HUV). This is not surprising. Even though it is based on basic physical principles the HIRHAM RCM has been refined over the years, e.g. in terms of convective parameterization and land-surface albedo, to better reproduce observations. Moreover, the model configuration (domain extent and grid size) used here was the best performing in terms of simulating precipitation and air temperature, as well as representing the atmospheric circulation patterns (Larsen et al., 2013). Likewise, MIKE SHE SWET has been subject to rigorous inverse modelling to assess parameter values (Larsen et al., submitted). By coupling, the existing land-surface scheme in HIRHAM is replaced by MIKE SHE SWET over the Skjern catchment. Calibration or parameter tuning of complex models comprising several processes often introduces compensational errors (i.e. providing the right answer for the wrong reason) in the different model components, in order to ensure that the model fits observational data as well as possible (Graham and Jacob, 2000). When the existing land-surface scheme in HIRHAM is replaced by MIKE SHE SWET, it will inevitably provide different results likely to be poorer in terms of a hindcast assessment. We should, however, highlight that the coupled system shows benefits over the uncoupled when assessing longer term periods such as cumulative precipitation where high frequency DTI's produce better results (figure 6). Also, greater accuracy in the representation of soil moisture and water available for evapotranspiration, in the coupled system, could explain these findings. In terms of future climate projections, which are typically in the range of 10-30 year integrations, this is very promising and suggests that there could be potential added value in using the coupled model system. Similar results, where the added complexity when joining two existing model

systems does not lead to obvious direct improvements in simulations, has also been seen in studies of coupling ocean models and atmosphere models (Covey et al., 2004).

From a different perspective the fact that the observed coupled model performance in many respects is poorer, when replacing the existing land-surface scheme with a more elaborate and well-calibrated one (MIKE SHE SWET), suggests that some of the HIRHAM components could be improved. So far very few attempts have been made in formalised calibration of RCMs, and we are not aware of any study that aims at calibrating coupled hydrology-RCM models. While there is a very interesting perspective here in a formal calibration of HIRHAM, e.g. as done by Bellprat et al. (2012), and in learning from the coupled model to improve the HIRHAM parameterisations, this is outside the scope of the current study.

4.2 – Data transfer interval (DTI)

As four out of six of the assessed climatic variables exhibit improved performance statistics with a lower DTI, the relation between computation time and DTI (figure 4) is highly relevant for studies over longer periods. This improved performance of the coupled setup is constrained, however, by a corresponding increase in computation time. The general decrease in RMSE levels with lower DTI is not surprising as a more frequent update of the surface forcing from MIKE SHE will include more dynamic features in the land-surface exchange and better align with variations in the surface energy balance affecting the land-atmosphere interaction. To fully capture the higher degree of dynamics in the land-surface-atmosphere interaction and dependence during unstable atmospheric conditions, a high frequency DTI closer to the RCM time step is likely to be important. One might suspect the effect of DTI to level off when approaching the internal HIRHAM model time step of 120 seconds and to obtain results affected by coupling features alone. Along these lines, a more dynamic pattern is seen for most variables for days with a higher degree of cloud cover and lower Rg levels (10 and 17 July) (figure 7).

Similar to this study Maxwell et al. (2011) have tested the timing of data transfer between the ParFlow hydrological model and the WRF atmospheric model in a 48 hour idealized constructed setup. The

simulations were performed by using four transfer intervals of 5, 10, 60 and 360 seconds, where WRF used a constant time step of 5 seconds (nonhydrostatic model) and the time step in ParFlow varied with the transfer interval. Good water balance results were obtained for transfer rates up to 12 times that of WRF (60 seconds) whereas the results for transfer interval of 360 second deteriorated. Even though a smaller time step was used in WRF than in HIRHAM in the present study (5 seconds compared to 120 seconds), the results of Maxwell et al. (2011) correspond reasonably well to our results, where a transfer rate of 12 times that of HIRHAM would correspond to a 24 min DTI.

4.3 - Impact of coupling evaluated against climate model variability

Climate models as proxies for real atmospheric conditions show considerable internal variability and the effects of introducing a full coupling therefore need to be evaluated on the basis of several simulations, where e.g. the initial boundary conditions are perturbed. In some cases the internal variability could be as large as effects introduced by the coupling of a regional climate model and a hydrology model. Hence, it is critically recommendable to explore variations caused by the physical changes (i.e. the coupling) as opposed to the internal climate model variation when developing coupled climate-hydrology modelling systems.

In our study the precipitation amounts spanning 75-99 mm and 52-134 mm for the HUV and CV simulations respectively, exhibit a significant variability in simulated PRECIP simply as a result of changes in the initial conditions. This has also been shown in several other studies (Casati et al., 2004; van de Beek et al., 2011; Larsen et al., 2013), which have highlighted the importance of considering climate model variability when assessing model performance In the present case the coupling is seen to inflate the variability of local precipitation as compared to the uncoupled climate model simulations even considering internal climate model variability. Since many climate models generally tend underestimate the variability of local precipitation thus providing unrealistic projections of e.g. extreme precipitation events, this is again a potentially promising feature of a coupled model system e.g. with respect to the representation of long-

446 term trends in precipitation for longer periods (multiple years) and in future climate projections, and will be
447 investigated in future studies.
448
449 **4.4 – Test domains**
450 There is a clear tendency for increased RMSE levels from the TI simulations with a higher degree of coupling
451 with the exception of Rg results (figure 3). An important consideration in this regard is, however, the
452 specific location of each of the domains within Denmark (figure 1). For the uncoupled HUV simulations, a
453 similar pattern of increased RMSE values is seen in PRECIP for the same test domains as for the TI
454 simulations. Therefore, it is not possible to directly relate the share of MIKE SHE influence on the HIRHAM
455 simulations to the results. An additional cause of the pattern of higher RMSE levels for test domains located
456 in central Jutland (Dom1 – Dom4) as compared to the eastern Dom5 could be related to certain
457 geographical biases in the precipitation as often seen in RCMs, including HIRHAM (Jacob et al., 2007;
458 Polanski et al., 2010). Corresponding biases for temperature have also been found (Kjellström et al., 2007;
459 Plavcová and Kyselý, 2011). Proximity to the coastline has also been shown to affect precipitation results
460 from HIRHAM (Larsen et al., 2013) and thereby the available water affecting the energy balance budget. In
461 this regard, the test domains Dom2 and specifically Dom3-Dom4 are located close to Ringkøbing Fjord,
462 which might contribute to the higher RMSE levels of these compared to Dom5.
463
464 **4.5 - Scale of variables**
465 An essential consideration is to assess at which spatial scale the atmospheric variables are affected by the
466 land-surface. The Skjern River catchment covers an area of approximately 70 km x 50 km, and our
467 hypothesis is that areas in the proximity of the catchment and up to 25 km downstream of the catchment
468 (in relation to the dominant wind direction) may be affected by the model coupling. This corresponds to
469 atmospheric scales from smaller mesoscale to microscale. It could be argued, however, that the effect of
470 the coupling, although tested on regional scales below 100 km, could likely be imposed regionally on top of

larger scale atmospheric phenomena such as larger mesoscale and synoptic scale features. In this regard it should be noted that global incoming solar radiation (Rg) which is by and large affected by cloud cover and therefore by upstream larger meso- and synoptic scale conditions, shows no effect of the coupling scenario, as the RSME pattern resembles a somewhat random pattern as a function of DTI, test domain and model variability (figure 3). Similarly surface pressure (Ps) would be connected with larger scale weather systems and sea surface temperatures (Køltzow et al., 2011) and is seen to be constrained, to some degree, by lateral boundary conditions (Seth and Georgi, 1998; Diaconescu et al., 2007; Leduc and Laprise, 2009) but is highly influenced by domain characteristics (Larsen et al., 2013). The variables RH, V and Ta all vary on spatial scales far below the resolution of HIRHAM and even MIKE SHE and the improved results with a more frequent DTI could therefore be anticipated to some extent. Also PRECIP, in particular convective rainfall, can be seen at grid scales below the HIRHAM resolution (Casati et al., 2004).

Another potential contribution to the performance comes from the fact that HIRHAM is a hydrostatic RCM with a convective scheme close to, or at, the threshold of its minimum resolution as also suggested in Larsen et al. (2013). Although, HIRHAM has been tested at similar spatial scales previously and was found to provide reasonable results, at very fine temporal scales the hydrostatic nature of HIRHAM could arguably contribute to the degree of variability seen for precipitation, and the 11 km resolution naturally has its limits compared to newer studies utilizing atmospheric model resolutions of a few kilometres such as Kendon et al. (2014). Conversely, the uncertainty related to, e.g. the location and timing of precipitation events, are in general much larger than the model resolution even for very high resolution non-hydrostatic models, particularly at the time scales of climate projections (Rasmussen et al., 2012). Hence, in practical terms, the HIRHAM-MIKE SHE setup explored in this paper represents a likely compromise in terms of delivering results of sufficient spatial representation for a number of problems in climate projection studies.

4.6 - Perspectives for further use

Computationally, we show that it is feasible to run simulations using coupled models dedicated to different types of computing systems, in this case a high performance computer and a personal computer. Moreover, we have demonstrated that transient coupled climate-hydrology simulations at the decadal scale or longer is well within reach. The present proto-type implements a number of technical decisions inherent to the computing environment available for this study and more work is needed in order to reduce computation times, e.g. implementation of a more efficient memory-based data transmission schemes as prescribed in the OpenMI standard. In its current form the coupling approach, however, may easily be generalized to other computing environments. In terms of further model development this work suggests that several steps may be undertaken to improve the coupled model performance. While we directly link model variables in the present study using an OpenMI interface, the present framework could easily be extended by imposing empirical downscaling and bias correction methods to further improve model compatibility across time and spatial scales.

5 – Conclusions

This study presents the performance of the fully two-way coupled setup between the HIRHAM RCM and the combined MIKE SHE/SWET hydrological and land-surface models. In particular, the influence of the data transfer interval between the models (DTI), the domain of coupling influence and the HIRHAM model variability, was assessed.

Of the six HIRHAM output climate variables, precipitation, relative humidity, wind speed and air temperature (PRECIP, RH, V and Ta) showed significant differences between simulations from perturbed runs of HIRHAM and perturbed runs of two-way coupled MIKE SHE-HIRHAM, as well as significant improvements in RMSE with a reduced DTI in the evaluated range of 12 to 120 min DTIs. The improvement for precipitation is highlighted with regard to the potential in the coupled setup as this is considered one of the most difficult variables to simulate. The global radiation and surface pressure variables (Rg and Ps) were shown to have little to no impact from the coupling. Little to no improvement in the MIKE SHE output

variables is seen for decreased DTI values as the improvement in latent heat flux (LE) is in the same range as the sensible heat flux (H) decline.

The uncoupled and coupled HIRHAM model variability, induced by perturbing the HIRHAM runs with varying starting dates, was shown to correspond to 47% and 46%, respectively, of the average improvements in RMSE and MAE for the four significant variables when going from a 120 min to a 12 min DTI. Similarly significant variations were seen in the simulated precipitation where the eight two-way fully coupled simulations with 12 to 120 min DTI values (TI) produced spans in precipitation during the one year period of 108-170 mm for the five test domains. Similarly, the uncoupled (HUV) and coupled (CV) simulations where model variability was induced by changing initial conditions showed precipitation spans of 75-99 mm and 52-134 mm respectively. For all of these, the resulting span increased with a higher degree of coupling. Part of this pattern may be attributed to well-known geographical HIRHAM bias over the central Jutland ridge. The HIRHAM model variability as transferred to the MIKE SHE model in the 60 min DTI CV simulations were substantially higher for discharge than for the LE, H or soil (G) heat fluxes.

In general, the coupled modeling results (TI and CV) are poorer than the uncoupled results (HUV) when assessed on a sub-daily to daily basis whereas longer term precipitation is better reproduced by more frequent DTI coupled simulations. The poorer short-term coupled performance is not surprising as each of the models over the years, also prior to this study, have been separately refined (convective scheme and land-surface energy balance) or calibrated to accurately reproduce observations. These calibrations are likely to have compensated for errors in the separate and complex model components to ensure a proper data fit. We suggest that the replacement of the land-surface scheme in HIRHAM, as introduced by MIKE SHE, and the change in data input in MIKE SHE, as introduced by HIRHAM, causes this deterioration. A potential calibration of the coupled setup is outside the time-frame and scope of the present paper, however we see a great potential for further improvements.

Acknowledgments

546 The present study was funded by grants from the Danish Strategic Research Council for the project
547 Hydrological Modelling for Assessing Climate Change Impacts at Different Scales (HYACINTS–
548 www.hyacints.dk) under contract no: DSF-EnMi 2104-07-0008 and the project Centre for Regional Change
549 in the Earth system (CRES – www.cres-centre.dk) under contract no: DSF-EnMi 09-066868. The present
550 study is made possible through a collaboration with the HOBE project (www.hobecenter.dk) funded by the
551 Villum Kann Rasmussen Foundation.

552

553 **References**

554 • Alexandru, A., R. D. Elia and Laprisé, R.: Internal Variability in Regional Climate Downscaling at the
555 Seasonal Scale. Mon. Weather Rev., 135, 3221-3238, doi: 10.1175/MWR3456.1, 2007.
556 • Allerup, P., Madsen, H. and Vejen F.: Standardværdier (1961-90) af Nedbørkorrektioner. Danish
557 Meteorological Institute Technical Report 98-10, 1998.
558 • Anyah, R. O., Weaver, C. P., Miguez.Macho, G., Fan, Y. and Robock, A. Incorporating water table
559 dynamics in climate modeling: 3. Simulated groundwater influence on coupled land-atmosphere
560 Variability. J. Geophys. Res., 113, DO7103, doi:10.1029/2007JD009087, 2008.
561 • Bellprat, O., Kotlarski, S., Lüthi, D. and Schär, C.: Objective calibration of regional climate models. J.
562 Geophys. Res., 117, doi:10.1029/2012JD018262, 2012.
563 • Butts, M., Drews, M., Larsen, M. A. D., Lerer, S., Rasmussen, S. H., Gross, J., Overgaard, J.,
564 Refsgaard, J. C., Christensen, O. B. and Christensen, J. H.: Embedding complex hydrology in the
565 regional climate system – dynamic coupling across different modelling domains. Submitted.
566 • Casati, B., Ross, G. and Stephenson, D. B.: A new intensity-scale approach for the verification of
567 spatial precipitation forecasts. Meteorol. Appl., 11, 141–154, doi:10.1017/S1350482704001239,
568 2004.
569 • Caya, D., and Laprise, R.: A semi-implicit semi-Lagrangian regional climate model: The Canadian
570 RCM. Mon. Weather Rev., 127, 341–362, 1999.

- Christensen, J. H., Christensen, O. B., Lopez, P., Meijgaard, E. van and Botzet, M.: The HIRHAM4 Regional Atmospheric Climate Model. Danish Meteorological Institute Technical Report 96-4, 1996.
- Christensen, O. B., Drews, M., Christensen, J. H., Dethloff, K., Ketelsen, K., Hebestadt, I. and Rinke, A.: The HIRHAM regional climate model version 5. Danish Meteorological Institute Technical Report 06-17, 2006.
- Covey, C., Achutarao, K.M., Gleckler, P.J., Phillips, T.J., Taylor, K.E. and Wehner, M.F.: Coupled ocean-atmosphere climate simulations compared with simulations using prescribed sea surface temperature: effect of a ‘‘perfect ocean’’. Glob. Planet. Chang., 41, 1-14, doi:10.1016/j.gloplacha.2003.09.003, 2004.
- Cui, X., Graf, H.-F., Langmann, B., Chen, W. and Huang, R.: Climate impacts of anthropogenic land use changes on the Tibetan Plateau. Glob. Planet. Chang., 54, 33–56, doi:10.1016/j.gloplacha.2005.07.006, 2006.
- Dai, Y., Zeng, X., Dickinson, R. E., Baker, I., Bonan, G. B., Bosilovich, M. G., Denning, A. S., Dirmeyer, P. A., Houser, P. R., Niu, G., Oleson, K. W., Schlosser, C. A., and Yang, Z-L.,: The common land model, Bull. Am. Meteorol. Soc., 84, 1013–1023, doi:10.1175/BAMS-84-8-1013, 2003
- Diaconescu, E. P., Laprise, R. and Sushama, L.: The impact of lateral boundary data errors on the simulated climate of a nested regional climate model. Clim. Dyn., 28, 333-350, doi:10.1007/s00382-006-0189-6, 2007
- Ek, M., Mitchell, K. E., Lin, Y., Rogers, E., Grunmann, P., Koren, V., Gayno, G. and Tarpley, J. D.: Implementation of Noah land surface model advances in the National Centers for Environmental Prediction operational mesoscale Eta model. J. Geophys. Res., 108, 8851, doi:10.1029/2002JD003296, 2003.
- Gerten, D., Schaphoff, S., Haberlandt, U., Lucht, W. and Sitch, S.: Terrestrial vegetation and water balance—hydrological evaluation of a dynamic global vegetation model. J. Hydrol., 286, 249–270, doi:10.1016/j.jhydrol.2003.09.029, 2004.

- Giorgi, F. and Bi, X.: A study of internal variability of a regional climate model. J. Geophys. Res., 105, 29503-29521, 2000.
- Goodall, J.L., Saint, K. D., Ercan, M. B., Briley, L. J., Murphy, S., You, H., DeLuca, C. and Rood, R. B.: Coupling climate and hydrological models: Interoperability through Web Services. Environ. Modell. Softw., 46, 250-259, doi: 10.1016/j.envsoft.2013.03.019, 2013.
- Graham, L. P. and Jacob, D.: Using large-scale hydrologic modeling to review runoff generation processes in GCM climate models. Meteorol. Z., 9, 49-57, 2000.
- Graham, D. N. and Butts, M. B.: Flexible, integrated watershed modelling with MIKE SHE, In Watershed Models, Eds. V.P. Singh & D.K. Frevert, 245-272, CRC Press. ISBN: 0849336090, 2005.
- Gregersen, J.B., Gijsbers, P. J. A., Westen, S. J. P. and Blind, M.: OpenMI: the essential concepts and their implications for legacy software. Adv. Geosci., 4, 37–44, doi:10.5194/adgeo-4-37-2005, 2005.
- Gregersen, J. B., Gijsbers, P. J. A. and Westen, S. J. P.: Open modelling interface. J. Hydroinform., 9, 175–191, doi:10.2166/hydro.2007.023, 2007.
- Højberg, A .L., Troldborg, L., Stisen, S., Christensen, B. S. B. and Henriksen, H. J.: Stakeholder driven update and improvement of a national water resources model. Environ. Modell. Softw., 40, 202-213, doi: 0.1016/j.envsoft.2012.09.010, 2013.
- Jacob, D., Bärring, L., Christensen, O. B., Christensen, J. H., De Castro, M., Déqué, M., Giorgi, F., Hagemann, S., Hirschi, M., Jones, R., Kjellström, E., Lenderink, G., Rockel, B., Sánchez, E., Schär, C., Seneviratne, S. L., Somot, S., Van Ulden, A. P. and Van Den Hurk, B. J. J. M.: An inter-comparison of regional climate models for Europe: model performance in present-day climate. Clim. Chang., 81, 31–52, doi:10.1007/s10584-006-9213-4, 2007.
- Jiang, X., Niu, G.-Y., Yang, Z.-L. Impacts of vegetation and groundwater dynamics on warm season precipitation over the Central United States. J. Geophys. Res., 114, DO6109, doi: 10.1029/2008JD010756, 2009.

- Kendon, E. J., Roberts, N. M., Fowler, H. J., Roberts, M. J., Chan, S. C and Senior, C. A. Heavier summer downpours with climate change revealed by weather forecast resolution model. Nat. Clim. Chang., 4, 570-576, doi:10.1038/NCLIMATE2258, 2014.
- Kjellström, E., Bärring, L., Jacob, D., Jones, R., Lenderink, G. and Schär, C.: Modelling daily temperature extremes: recent climate and future changes over Europe. Clim. Chang., 81, 249–265, doi:10.1007/s10584-006-9220-5, 2007.
- Kollet, S. J. and Maxwell, R. M.: Capturing the influence of groundwater dynamics on land surface processes using an integrated, distributed watershed model. Water Resour. Res., 44, doi:10.1029/2007WR006004, 2008.
- Kunstmann, H. and Stadler, C. High resolution distributed atmospheric-hydrological modelling for Alpine catchments. J. Hydrol., 314, 105-124, doi:10.1016/j.jhydrol.2005.03.033, 2005.
- Køltzow, M. A. Ø., Iversen, T. and Haugen, J. E.: The Importance of Lateral Boundaries, Surface Forcing and Choice of Domain Size On the role of domain size and resolution in the simulations for Dynamical Downscaling of Global Climate Simulations. Atmosphere, 2, 67–95, doi:10.3390/atmos2020067, 2011.
- Larsen, M. A. D., Thejll, P., Christensen, J. H., Refsgaard, J. C. and Jensen, K. H.: On the role of domain size and resolution in the simulations with the HIRHAM region climate model. Clim. Dyn., 40, 2903-2918, doi:10.1007/s00382-012-1513-y, 2013.
- Larsen, M. A. D., Refsgaard, J. C., Jensen, K. H., Butts, M. B., Stisen, S. and Mollerup, M.: Calibration of a distributed hydrology and land surface model using uncertain energy flux measurements. Water Resour. Res., submitted.
- Leduc, M., Laprise, R.: Regional climate model sensitivity to domain size. Clim. Dyn., 32, 833-854, doi:10.1007/s00382-008-0400-z, 2009.

643 • Maxwell, R. M., Chow, F. K. and Kollet, S. J.: The groundwater–land-surface–atmosphere
644 connection: Soil moisture effects on the atmospheric boundary layer in fully-coupled simulations.
645 Adv. Water Resour., 30, 2447–2466, doi:10.1016/j.advwatres.2007.05.018, 2007.
646 • Maxwell, R. M., Lundquist, J. K., Mirocha, J. D., Smith, S. G., Woordward, C. S. and Tompson, A. F.
647 B.: Development of a Coupled Groundwater–Atmosphere Model. Mon. Weather Rev., 39, 96-116,
648 doi: 10.1175/2010MWR3392.1, 2011.
649 • Overgaard, J.: Energy-based land-surface modelling: new opportunities in integrated hydrological
650 modeling, Ph.D. Thesis, Institute of Environment and Resources, DTU, Technical University of
651 Denmark, 2005.
652 • Plavcová, E. and Kyselý, J.: Evaluation of daily temperatures in Central Europe and their links to
653 large-scale circulation in an ensemble of regional climate models. Tellus A, 63, 763–781,
654 doi:10.1111/j.1600-0870.2011.00514.x, 2011.
655 • Polanski, S., Rinke, A. and Dethloff, K.: Validation of the HIRHAM-Simulated Indian Summer
656 Monsoon Circulation. Adv. Meteorol., 2010, doi:10.1155/2010/415632, 2010.
657 • Rasmussen, S. H.: Modelling land surface - atmosphere interactions. Ph.D. Thesis, University Of
658 Copenhagen, Department Of Geography and Geology, 2012.
659 • Rasmussen, S.H., Christensen, J.H., Drews, M., Gochis, D. and Refsgaard, J.C.: Spatial-Scale
660 Characteristics of Precipitation Simulated by Regional Climate Models and the Implications for
661 Hydrological Modeling. J. Hydrometeor, 13, 1817–1835, doi:10.1175/JHM-D-12-07.1, 2012.
662 • Rihani, J. F.: Isolating Effects of Water Table Dynamics, Terrain, and Soil Moisture Heterogeneity on
663 the Atmospheric Boundary Layer Using Coupled Models. Ph.D. Thesis, Civil and Environmental
664 Engineering, University of California, Berkeley, USA, 2010.
665 • Ringgaard, R., Herbst, M., Friborg, T. and Soegaard, H. Energy Fluxes above Three Disparate
666 Surfaces in a Temperate Mesoscale Coastal Catchment. Vadose Zone J., 10, 54–66,
667 doi:10.2136/vzj2009.0181, 2011.

- Ringgaard, R.: On variability of evapotranspiration - The role of surface type and vegetation. Ph.D. Thesis, University Of Copenhagen, Department Of Geography and Geology, 2012.
- Roeckner, E., Bäuml, G., Bonaventura, L., Brokopf, R., Esch, M., Giorgetta, M., Hagemann, S., Kirchner, I., Kornblueh, L., Manzini, E., Rhodin, A., Schlese, U., Schulzweida U. and Tompkins, A.: Part 1. Model description. The atmospheric general circulation model ECHAM5. Report no. 349, Max-Planck-Institut fürMeteorologie (MPI-M), 2003.
- Seneviratne, S. I., Lüthi, D., Litschi, M. and Schär, C.: Land–atmosphere coupling and climate change in Europe. Nature, 443, 205-209, doi:10.1038/nature05095, 2006.
- Seth, A. and Giorgi, F.: The effect of domain choice on summer precipitation simulation and sensitivity in a regional climate model. J. Clim., 11, 2698–2712, 1998.
- Shresta, P., Sulis, M., Masbou, M., Kollet, S. and Simmer, C. A scale-consistent Terrestrial Systems Modeling Platform based on COSMO, CLM and ParFlow. Mon. Weather Rev., (accepted but not numbered), 2014.
- Shuttleworth, W. J. and Wallace, J. S.: Evaporation from sparse crops – an energy combination theory. Q. J. Roy. Meteor. Soc., 111, 839-855, 1985.
- Skamarock, W. C., Klemp, J. B., Dudhia, J., Gill, O. D., Barker, D. M., Duda, M. G., Huang, X., Wang, W. and Powers, J. G.: A description of the Advanced Research WRF version 3, NCAR Techical Note NCAR/TN-4751STR, Boulder, Colorado, USA, 2008.
- Smiatek, G., Kunstmann, H. and Werhahn, J. Implementation and performance analysis of a high resolution coupled numerical weather and river runoff prediction model system for an Alpine catchment. Environ. Modell. Softw., 38, 231-243, doi:10.1016/j.envsoft.2012.06.001, 2012.
- Stisen, S., McCabe, M. F., Refsgaard, J. C., Lerer, S. and Butts, M. B.: Model parameter analysis using remotely sensed pattern information in a multi-constraint framework, J. Hydrol., 409, 337–349, doi:10.1016/j.jhydrol.2011.08.030, 2011a.

692 • Stisen, S., Sonnenborg, T., Højberg, A. L., Troldborg, L. and Refsgaard, J. C.: Evaluation of Climate
693 Input Biases and Water Balance Issues Using a Coupled Surface–Subsurface Model. Vadose Zone J.,
694 10, 37–53, doi:10.2136/vzj2010.0001, 2011b.
695 • Stisen, S., Højberg, A. L., Troldborg, L., Refsgaard, J. C., Christensen, B. S. B., Olsen, M. and
696 Henriksen, H. J.: On the importance of appropriate precipitation gauge catch correction for
697 hydrological modelling at mid to high latitudes. Hydrol. Earth Syst. Sci., 16, 4157–4176,
698 doi:10.5194/hess-16-4157-2012, 2012.
699 • Undén, P., Rontu, L. Järvinen, H., Lynch, P., Calvo, J. and co-authors.: HIRLAM-5 scientific
700 documentation. HIRLAM Report, SMHI, SE-601 76 Norrköping, Sweden, 144 p, 2012.
701 • Uppala, S., Dee, S., Kobayashi, S., Berrisford, P. and Simmons, A.: Towards a climate data
702 assimilation system: status update of ERA-Interim. ECMWF Newsletter No. 115, 12–18, 2008.
703 • van de Beek, C. Z., Leijnse, H., Torfs, P. J. J. F. and Uijlenhoet, R.: Climatology of daily rainfall semi-
704 variance. Hydrol. Earth. Syst. Sci., 15, 171–183, doi:10.5194/hess-15-171-2011, 2011.
705 • Xue, M., Droegemeier, K. K. and Wong, V.: The advanced regional prediction system (ARPS), A
706 multi-scale non-hydrostatic atmospheric simulation and prediction model. Part I: model dynamics
707 and verification. Meteorol. Atmos. Phys., 75, 161–93, 2000.
708 • Xue, M., Droegemeier, K. K., Wong, V., Shapiro, A., Brewster, A., Carr, F., Weber, D., Liu, Y. and
709 Wang, D.: The advanced regional prediction system (ARPS), a multi-scale non-hydrostatic
710 atmospheric simulation and prediction tool. Part II: model physics and applications. Meteorol.
711 Atmos. Phys., 76, 143–65, 2001.
712 • Yan, H., Wang, S. Q., Billesbach, D., Oechel, W., Zhang, J. H., Meyers, T., Martin, T. A., Matamala, R.,
713 Baldocchi, D., Bohrer, G., Dragoni, D. and Scott, R.: Global estimation of evapotranspiration using a
714 leaf area index-based surface energy and water balance model. Remote. Sens. Environ., 124, 581–
715 595, doi:10.1016/j.rse.2012.06.004, 2012.

- York, J. P., Person, M., Gutowski, W. J. and Winter, T. C. Putting aquifers into atmospheric simulation models: an example from the Mill Creek Watershed, northeastern Kansas. Adv. Water Resour., 25, 221-238, 2002.
- Zabel, F. and Mauser, W.: 2-way coupling the hydrological land surface model PROMET with the regional climate model MM5. Hydrol. Earth Syst. Sci., 17, 1705–1714, doi:10.5194/hess-17-1705-2013, 2013.
- Zeng X.-M., Zhao, M., Su, B.-K., Tang, J.-P., Zheng, Y.-Q., Zhang, Y.-J. and Chen, J.: Effects of the land-surface heterogeneities in temperature and moisture from the ‘‘combined approach’’ on regional climate: a sensitivity study. Glob. Planet. Chang., 37, 247–263, doi:10.1016/S0921-8181(02)00209-6, 2003.

	Simulation group name	No. of runs	Description	HIRHAM	MIKE SHE
Coupled simulations	TI	8	Fully two-way coupled, DTI's of 12, 15, 24, 30, 48, 60, 90 and 120 min	x	x
	CV	8	Fully two-way coupled, DTI's of 60 min, perturbed initial conditions (simulations start between 1-8. May)	x	x
One-way or uncoupled simulations	HUV	8	HIRHAM runs alone, perturbed initial conditions (simulations start between 1-8. May)	x	
	MSDS	2	Two MIKE SHE runs with 1) observation data forcing and 2) with HIRHAM forcing through a one-way coupling		x

Table 1.

	Variable	MAE absolute change	MAE percentage change	MAE CV variability	MAE HUV variability	RMSE absolute change	RMSE percentage change	RMSE CV variability	RMSE HUV variability
HIRHAM output variables	**PRECIP (mm/day)**	0.3	8.3	0.2	0.2	1.1	16.4	0.7	0.6
	RH (%)	0.8	7.9	0.3	0.1	1.1	8	0.3	0.2
	V (m/s)	0.1	5.4	0.0	0.0	0.2	5.8	0.5	0.1
	Rg (W/m^2)	-0.1	-0.2	2.6	1.3	-0.1	-0.1	6.0	3.2
	Ta (^oC)	0.2	10.1	0.1	0.1	0.3	8.8	0.1	0.2
	Ps (hPa)	0.0	1.8	0.1	0.1	0.1	2.7	0.2	0.2
MIKE SHE output variables	**LE (W/m^2)**	1.9	6.9	0.9	-	1.9	4.5	1.5	-
	H (W/m^2)	-2.3	-7.4	0.5	-	-3.1	-6	1.5	-
	G (W/m^2)	-0.1	-3.1	0.2	-	-0.7	-7.9	0.7	-
	Q (W^3/s)	-0.4	-12.2	0.7	-	0.1	-0.1	2.2	-

Table 2.

731 Figure 1. Location of HIRHAM regional climate domain within Europe, MIKE SHE catchment within Denmark, three
732 point measurement sites, and location of five evaluation domains.
733
734 Table 1. Simulation outline showing simulation groups, number of runs in each group and short description of
735 simulation group characteristics. The two latter columns show from which of the two model components the
736 simulation output derives.
737
738 Figure 2. Flow chart of the data flow and analyses performed in the present study and a legend of the variables
739 mentioned in the study.
740
741 Figure 3. HIRHAM output RMSE statistics for each of the test domains for the coupled TI simulations. Linear trend lines
742 are shown with RMSE as a function of DTI as well as the average trend line correlation coefficients where the
743 significant correlations on a two-sided 95% confidence level are underlined.
744
745 Figure 4. Model execution time in hours of wall time as a function of DTI. DTI steps of 6, 9, 12, 15, 24, 30, 48, 60, 90
746 (eight CV runs), and 120 min were used whereas 6 and 9 min DTI values were extrapolated from unfinished runs. For
747 comparison the dashed line is the execution time for the uncoupled HIRHAM runs (HUV). The figure originates from
748 Butts et al. (2013).
749
750 Figure 5. RMSE variability for the TI, HUV and CV simulations for each of the five test domains. The dots represent the
751 median value, the box plots represent the 25-75th percentiles and the whiskers represent the entire data range.
752
753 Table 2. Absolute and percentage change in MAE and RMSE between the largest (120 min) and smallest (12 min) DTI
754 based on the average value of the linear trendlines of either the five test domains (HIRHAM output) or the
755 measurement sites (MIKE SHE output). Also shown is the absolute variability from the CV and HUV runs defined as the
756 minimum value subtracted from the maximum for the 60 min DTI averaged between test domains (HIRHAM output)
757 or measurement sites (MIKE SHE output) for each tested variable.
758

759 Figure 6. Precipitation sum curve for the evaluation period 1 May 2009 to 30 April 2010 for the five test domains and
760 the TI, HUV and CV simulations as well as the observations. Also given are the simulated mean values, the span in the
761 period sum for each plot group (minimum value subtracted from maximum value) and the observed mean values.
762
763 Figure 7. The six HIRHAM output variables assessed in the present study in the 10-17 July period (precipitation is 1-31
764 August to match the period in figure 9 with a higher dynamic in discharge) for all 24 TI, HUV and CV runs and for Dom1
765 (nine cell mean). The legend colouring reflects the overall simulation group (TI, HUV or CV) whereas each simulation is
766 in the colour shade as in figure 6.
767
768 Figure 8. MIKE SHE output RMSE statistics for each of the three flux tower measurement sites and the three discharge
769 stations for the TI, MSDS and CV simulations. For the TI simulations linear trendlines are shown with RMSE as a
770 function of DTI as well as the average trendline correlation coefficients where significant correlations on a two-sided
771 95% confidence level are underlined. Also, the variability of the perturbed CV simulations is shown.
772
773 Figure 9. Four MIKE SHE output variables for the period 10-17 July (discharge is 1-31 August) for the TI, CV and MSDS
774 runs and for Dom1 (nine cell mean). The legend colouring reflects the overall simulation group (TI, CV and MSDS) and
775 each simulation has the same colour shade as in figure 6. The individual flux sites are shown for LE only. Notice the y-
776 axis shifts to accommodate more sites.
777
778
779

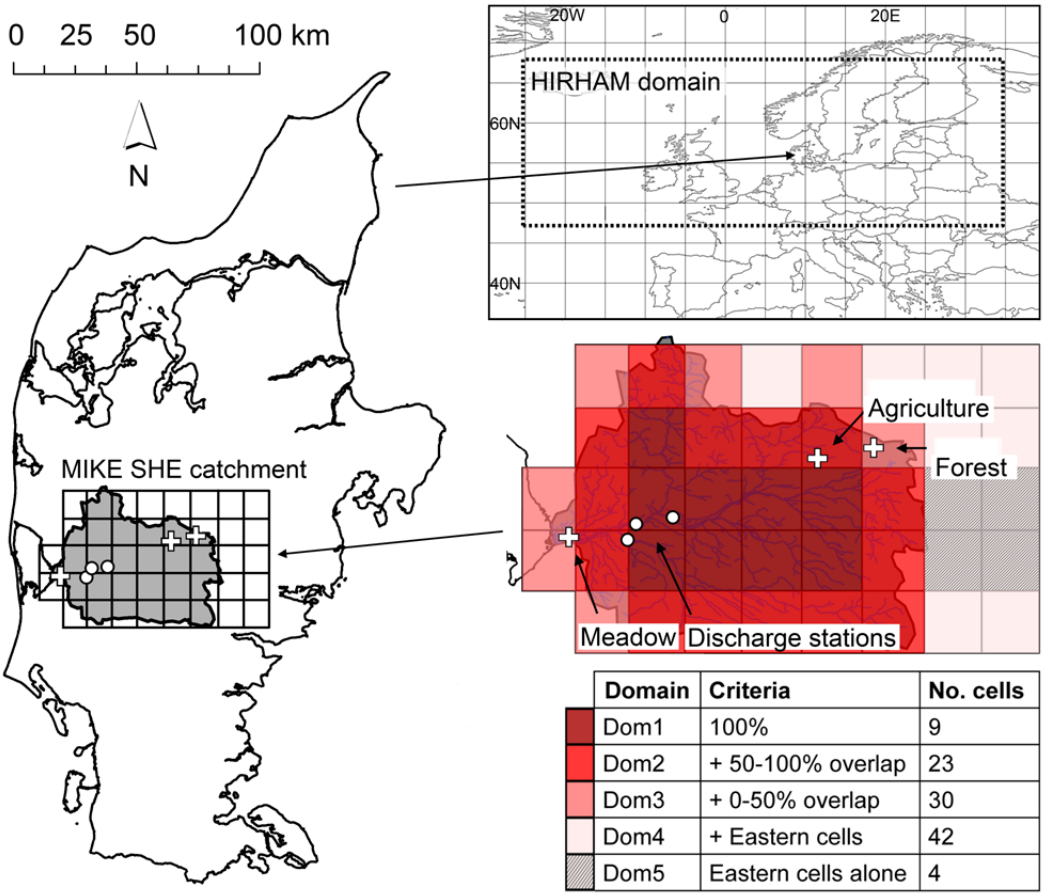

Domain	Criteria	No. cells
Dom1	100%	9
Dom2	+ 50-100% overlap	23
Dom3	+ 0-50% overlap	30
Dom4	+ Eastern cells	42
Dom5	Eastern cells alone	4

780

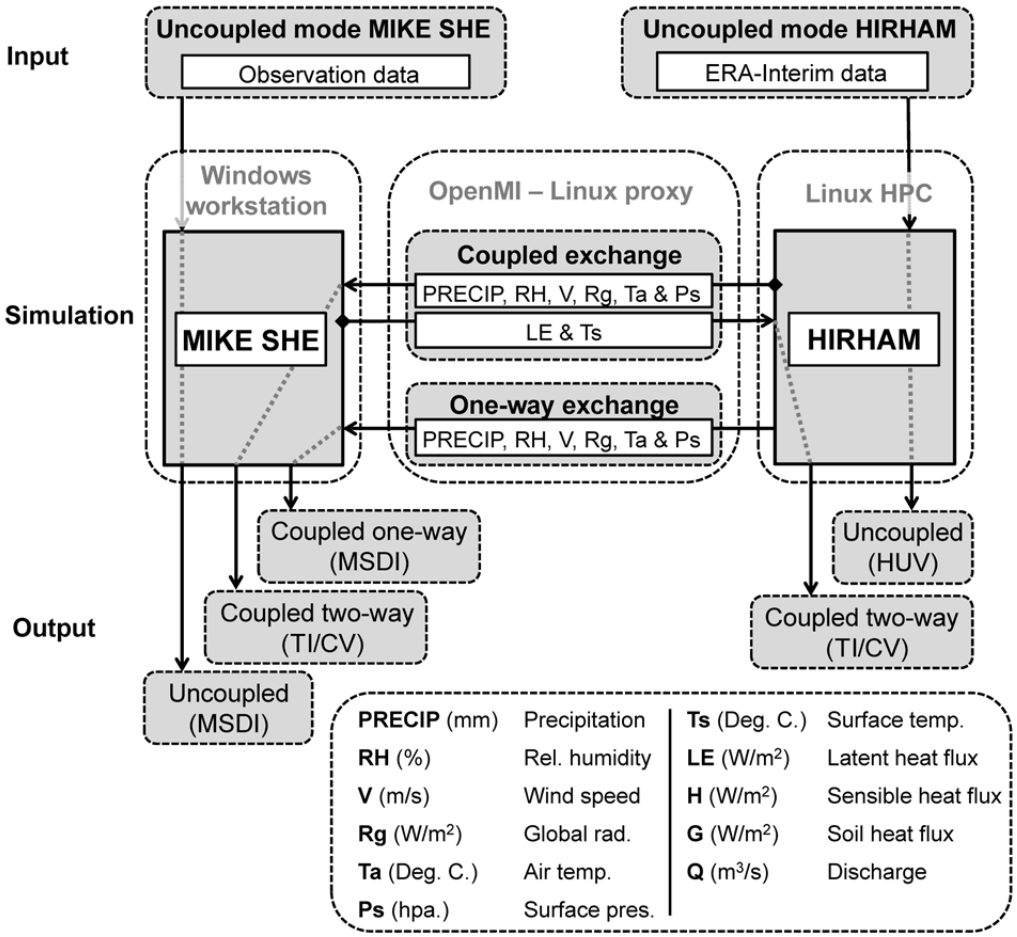
Input
Simulation
Output
Uncoupled mode MIKE SHE
Observation data
Uncoupled mode HIRHAM
ERA-Interim data
Windows workstation
OpenMI – Linux proxy
Linux HPC
Coupled exchange
PRECIP, RH, V, Rg, Ta & Ps
LE & Ts
One-way exchange
PRECIP, RH, V, Rg, Ta & Ps
MIKE SHE
HIRHAM
Coupled one-way (MSDI)
Coupled two-way (TI/CV)
Uncoupled (MSDI)
Uncoupled (HUV)
Coupled two-way (TI/CV)
PRECIP (mm) Precipitation
RH (%) Rel. humidity
V (m/s) Wind speed
Rg (W/m2) Global rad.
Ta (Deg. C.) Air temp.
Ps (hpa.) Surface pres.
Ts (Deg. C.) Surface temp.
LE (W/m2) Latent heat flux
H (W/m2) Sensible heat flux
G (W/m2) Soil heat flux
Q (m3/s) Discharge

781

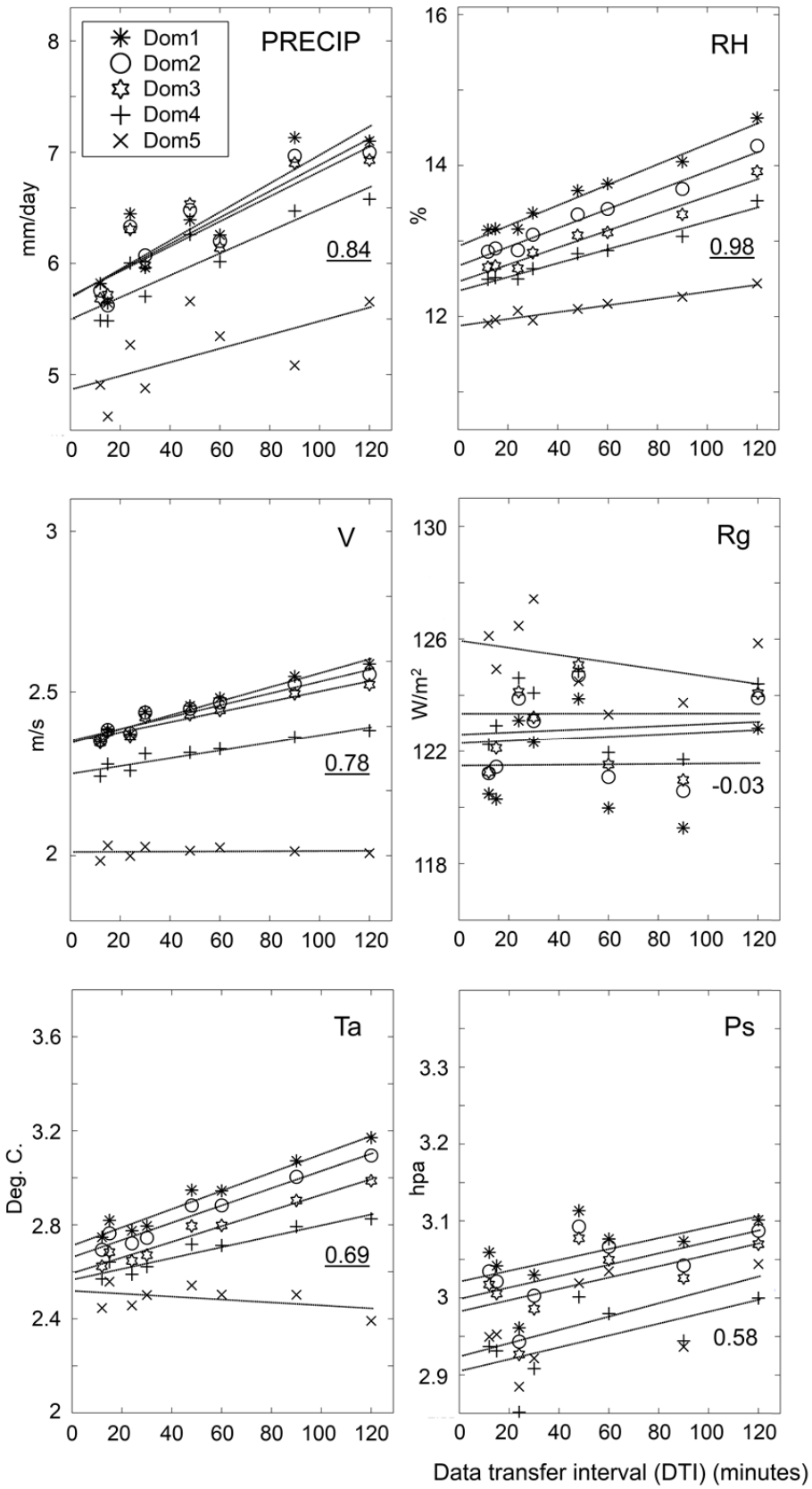
Dom1
Dom2
Dom3
Dom4
Dom5
PRECIP
mm/day
0.84
RH
%
0.98
V
m/s
0.78
Rg
W/m²
-0.03
Ta
Deg. C.
0.69
Ps
hpa
0.58
Data transfer interval (DTI) (minutes)

782

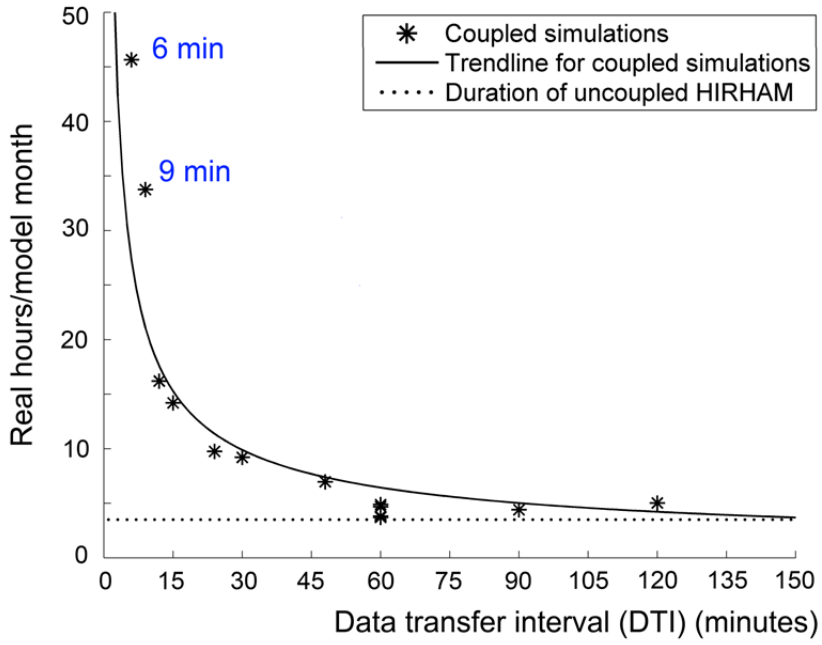
Coupled simulations
Trendline for coupled simulations
Duration of uncoupled HIRHAM
6 min
9 min
Real hours/model month
Data transfer interval (DTI) (minutes)
0
10
20
30
40
50
0
15
30
45
60
75
90
105
120
135
150

783

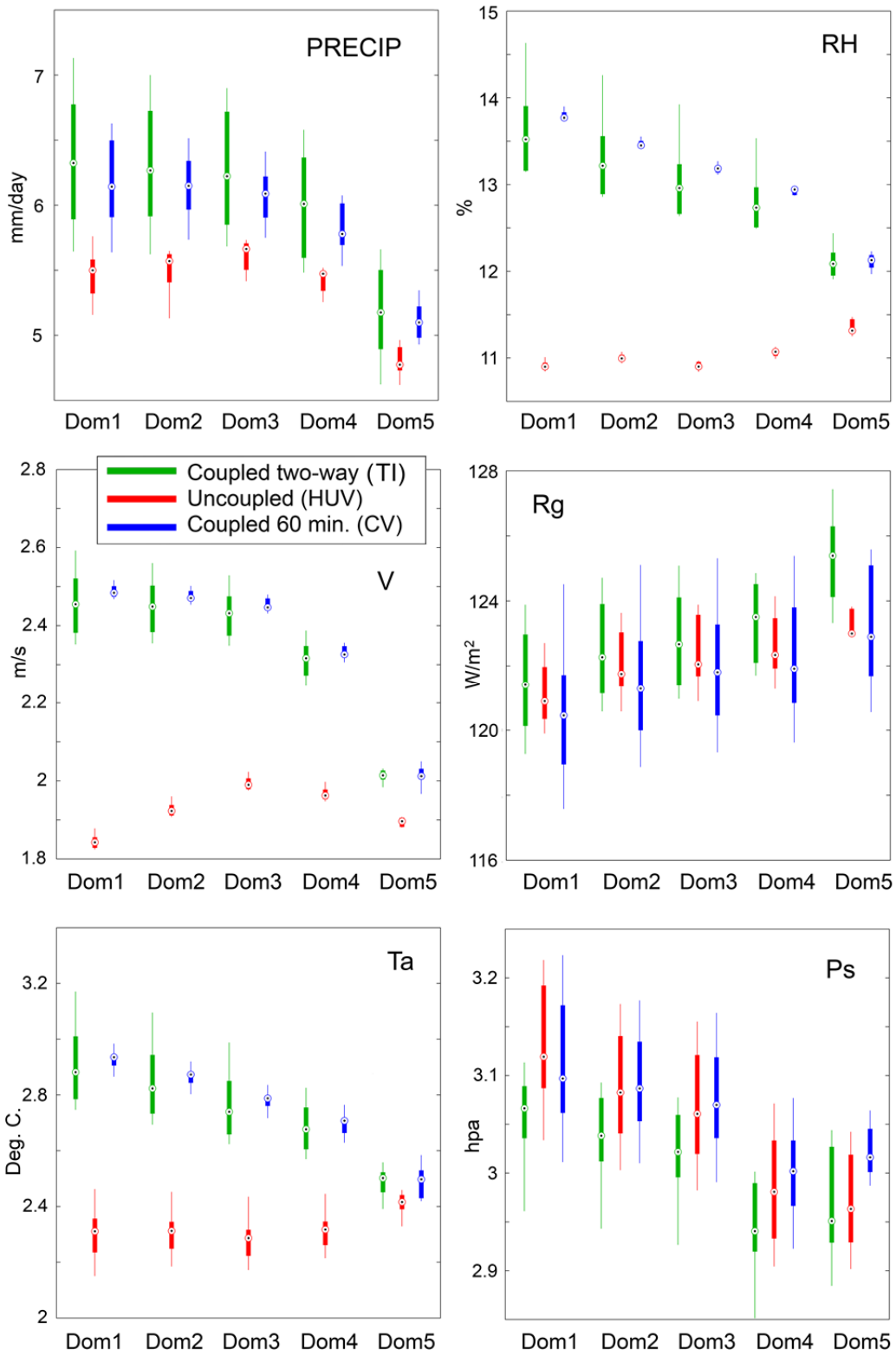
PRECIP
mm/day
7
6
5
Dom1
Dom2
Dom3
Dom4
Dom5
RH
%
15
14
13
12
11
Coupled two-way (TI)
Uncoupled (HUV)
Coupled 60 min. (CV)
V
m/s
2.8
2.6
2.4
2.2
2
1.8
Rg
W/m²
128
124
120
116
Ta
Deg. C.
3.2
2.8
2.4
2
Ps
hpa
3.2
3.1
3
2.9

784

785

786

787

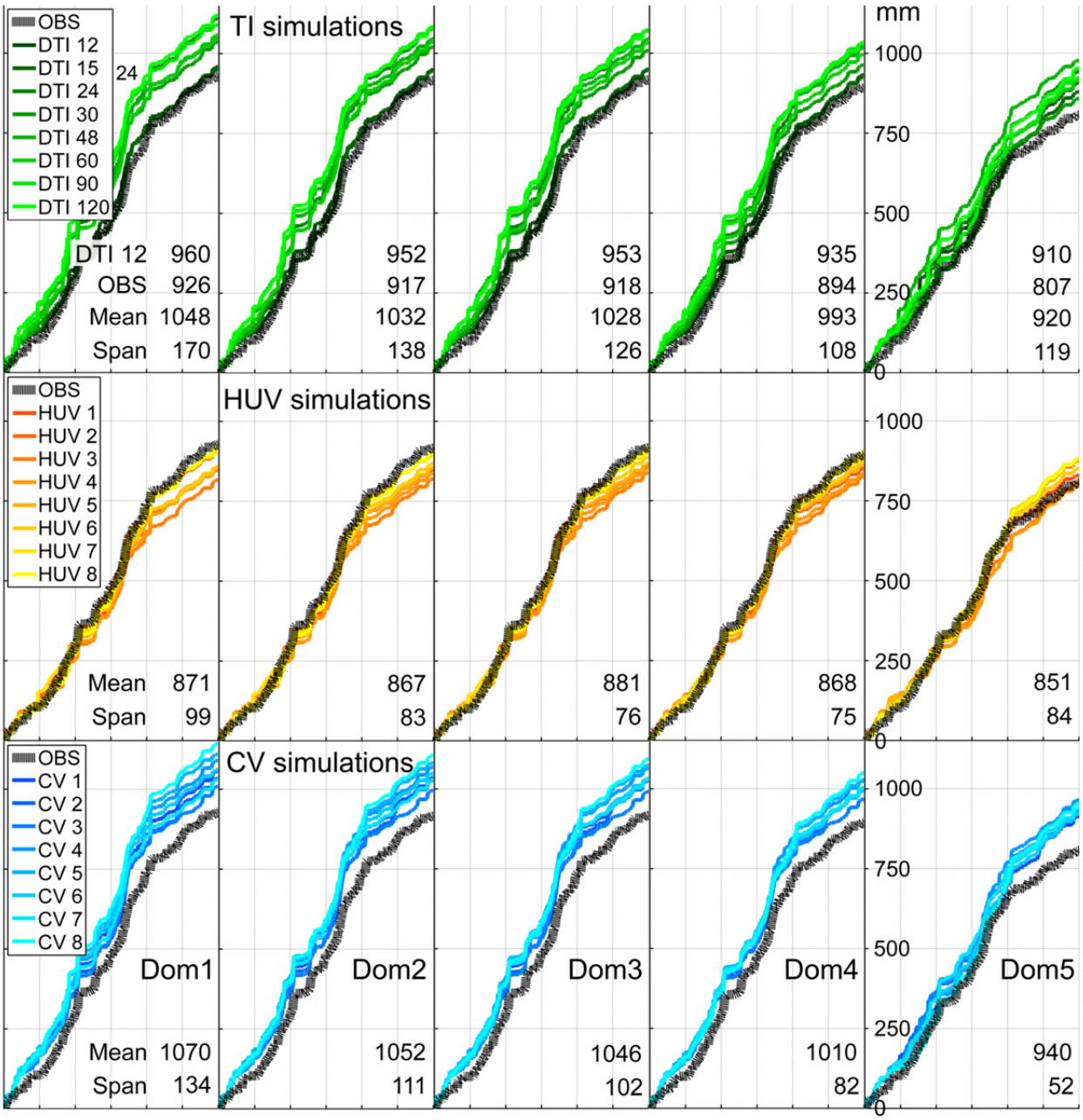
OBS
DTI 12
DTI 15
DTI 24
DTI 30
DTI 48
DTI 60
DTI 90
DTI 120
24
TI simulations
mm
1000
750
500
250
0
DTI 12 960
OBS 926
Mean 1048
Span 170
952
917
1032
138
953
918
1028
126
935
894
993
108
910
807
920
119
OBS
HUV 1
HUV 2
HUV 3
HUV 4
HUV 5
HUV 6
HUV 7
HUV 8
HUV simulations
Mean 871
Span 99
867
83
881
76
868
75
851
84
OBS
CV 1
CV 2
CV 3
CV 4
CV 5
CV 6
CV 7
CV 8
CV simulations
Dom1
Mean 1070
Span 134
Dom2
1052
111
Dom3
1046
102
Dom4
1010
82
Dom5
940
52

788

789

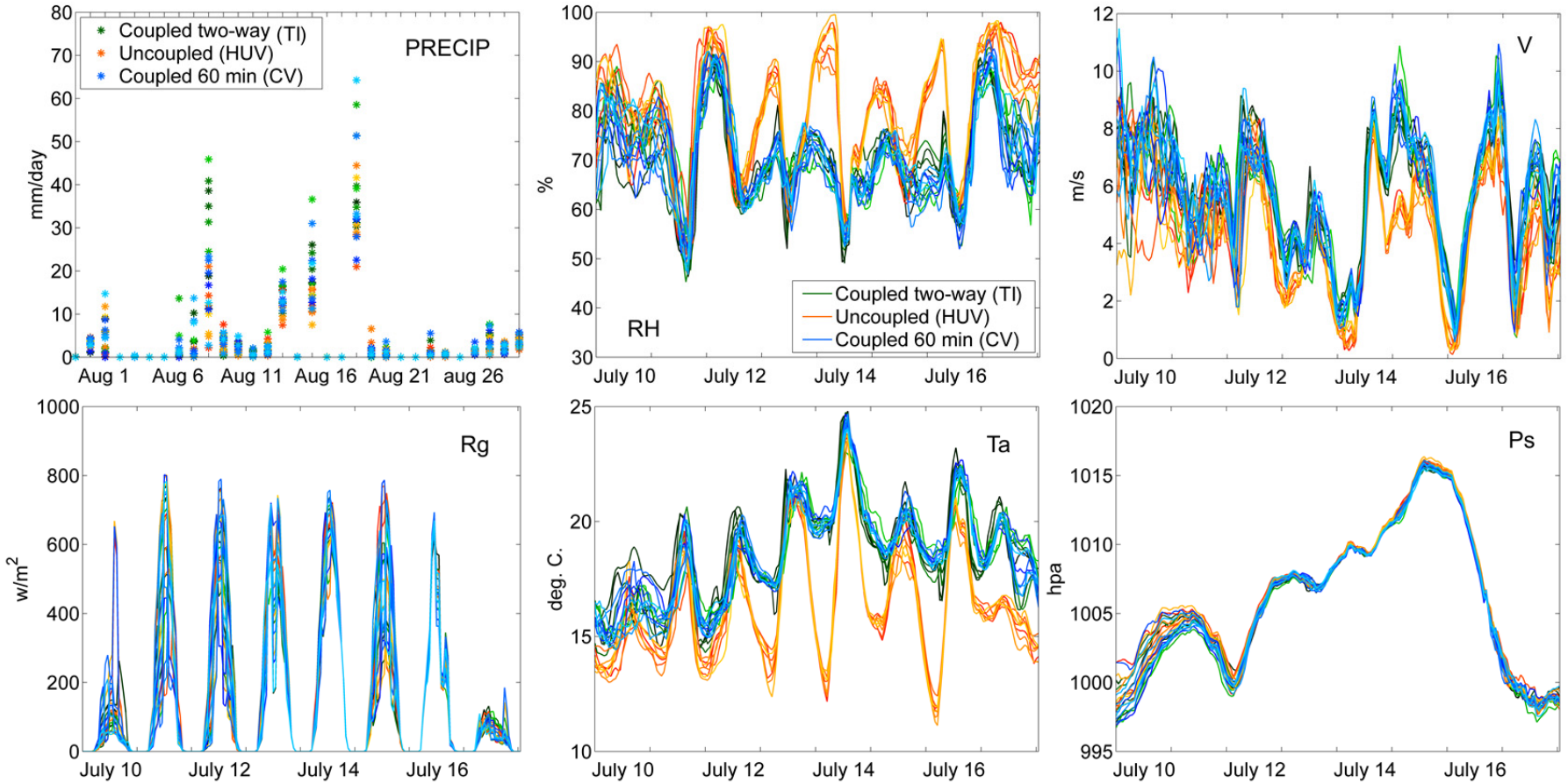
Coupled two-way (TI)
Uncoupled (HUV)
Coupled 60 min (CV)
PRECIP
mm/day
Aug 1
Aug 6
Aug 11
Aug 16
Aug 21
aug 26
RH
%
July 10
July 12
July 14
July 16
V
m/s
Rg
w/m2
Ta
deg. C.
Ps
hpa

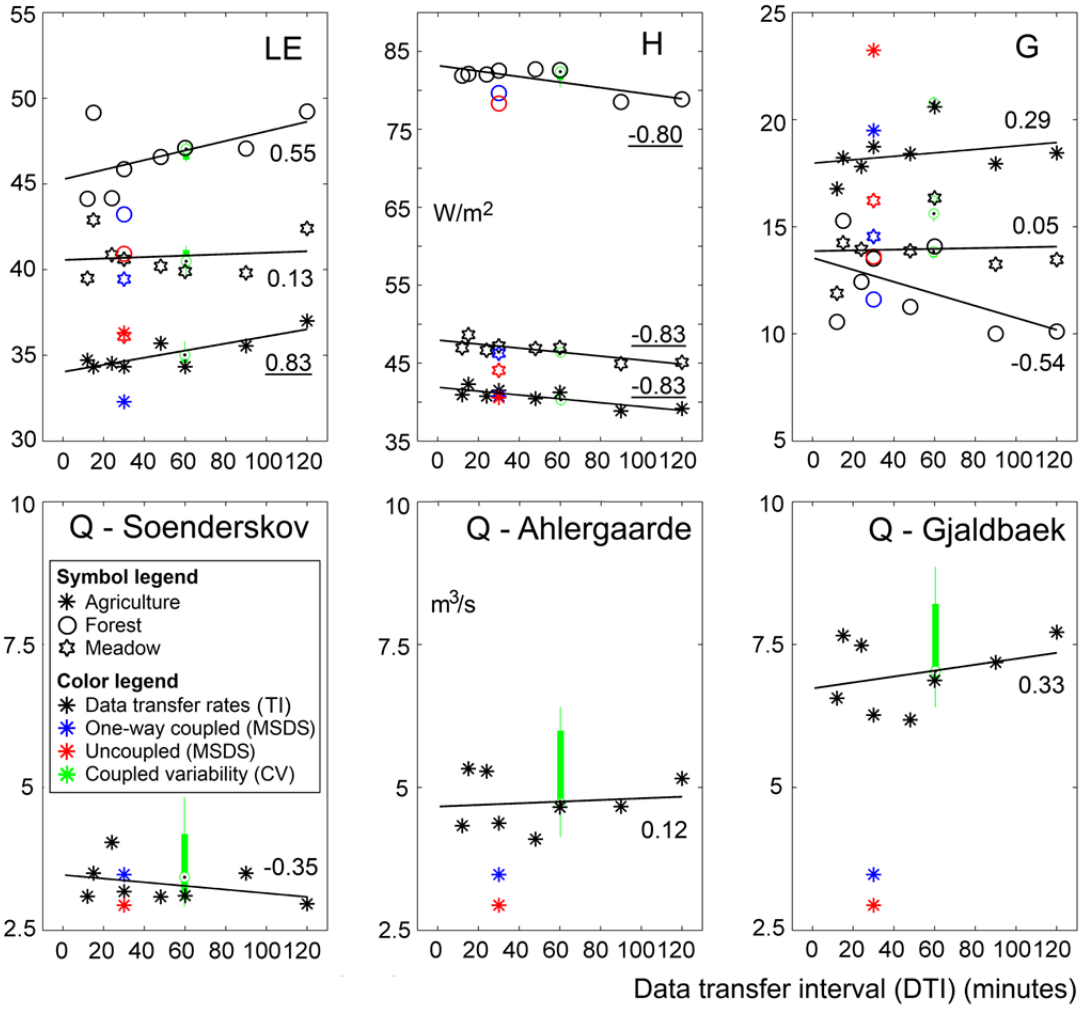
LE
0.55
0.13
0.83
H
W/m2
-0.80
-0.83
-0.83
G
0.29
0.05
-0.54
Q - Soenderskov
Symbol legend
Agriculture
Forest
Meadow
Color legend
Data transfer rates (TI)
One-way coupled (MSDS)
Uncoupled (MSDS)
Coupled variability (CV)
-0.35
Q - Ahlergaarde
m3/s
0.12
Q - Gjaldbaek
0.33
Data transfer interval (DTI) (minutes)

792

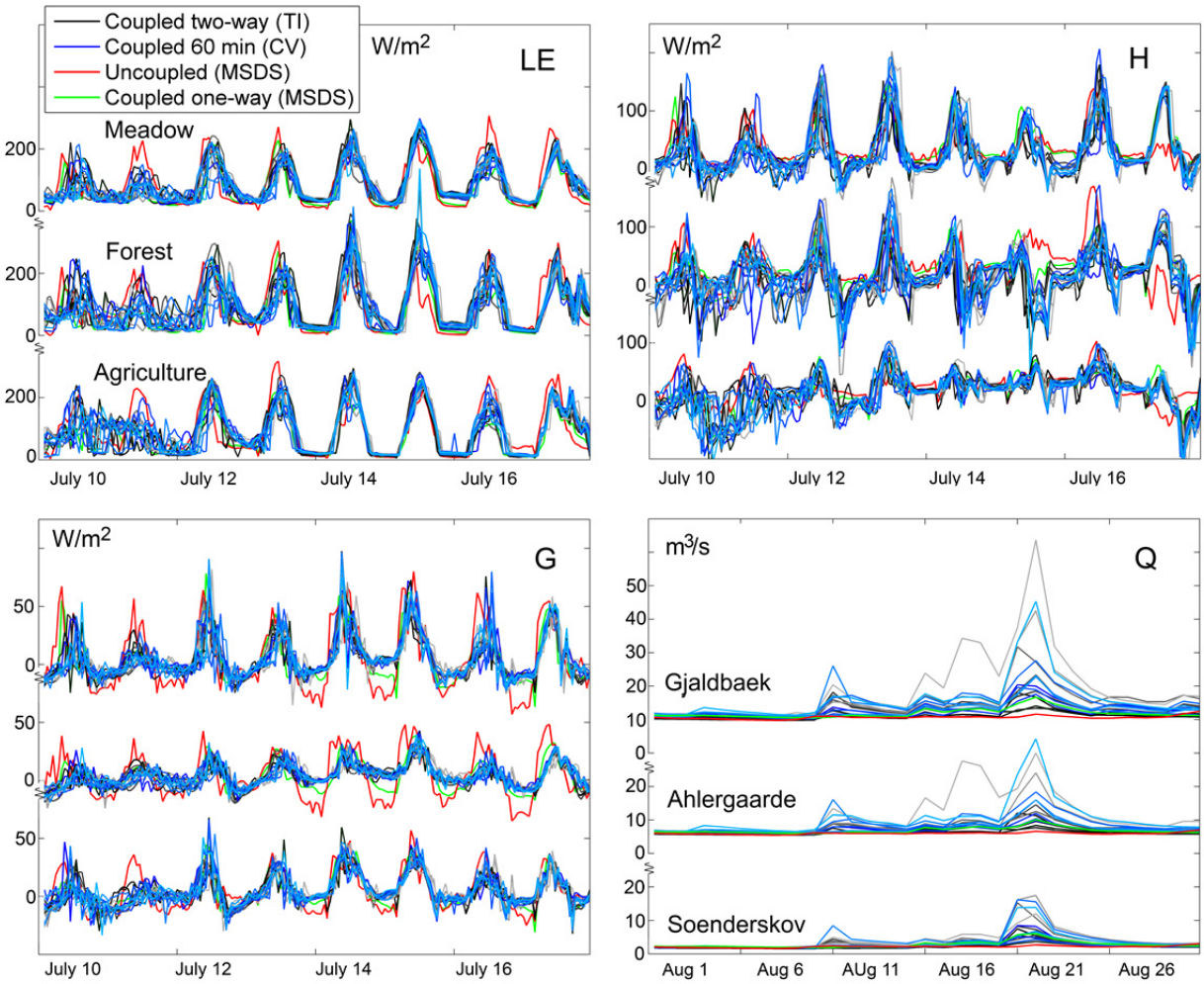
Coupled two-way (TI)
Coupled 60 min (CV)
Uncoupled (MSDS)
Coupled one-way (MSDS)
W/m2
LE
Meadow
Forest
Agriculture
200
0
July 10
July 12
July 14
July 16
W/m2
H
100
0
July 10
July 12
July 14
July 16
W/m2
G
50
0
July 10
July 12
July 14
July 16
m3/s
Q
Gjaldbaek
Ahlergaarde
Soenderskov
50
40
30
20
10
0
Aug 1
Aug 6
AUg 11
Aug 16
Aug 21
Aug 26

793

794